Wavelength-dependency of the impact of light on proliferation and DNA damage of corneal cells in vitro

Alicia Torriglia

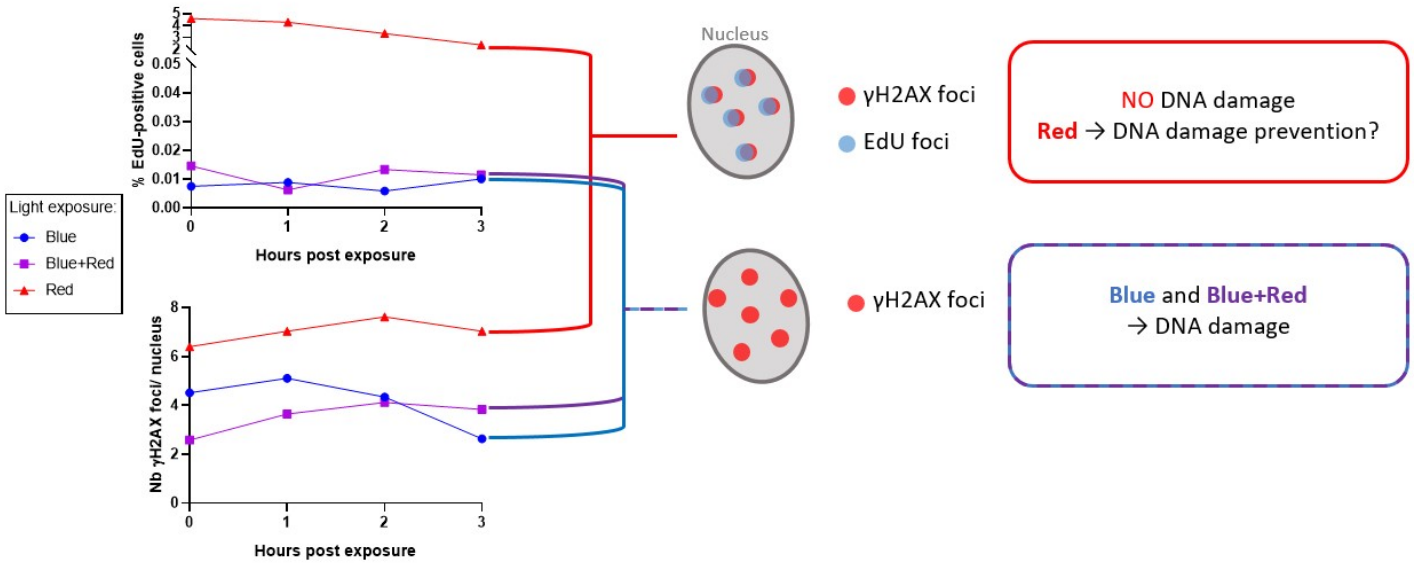
Light exposure:
Blue
Blue+Red
Red
% EdU-positive cells
Hours post exposure
Nb γH2AX foci/ nucleus
Hours post exposure
Nucleus
γH2AX foci
EdU foci
γH2AX foci
NO DNA damage
Red → DNA damage prevention?
Blue and Blue+Red
→ DNA damage

Wavelength-dependency of the impact of light on proliferation and DNA damage of corneal cells *in vitro*.

Anaïs Françon[a], Francine Behar-Cohen[a,b] and Alicia Torriglia[a]

Affiliations:

[a]Centre de Recherche des Cordeliers, INSERM UMRS 1138, Université Paris Cité, Sorbonne Université. Team:Physiopathology of OcularDiseases: Therapeutic Innovations. 15, rue de l'école de Médecine 75006 Paris, France.

[b] Assistance Publique, Hôpitaux de Paris, Hôpital Cochin, Ophtalmopole, 27, rue du Faubourg Saint-Jacques 75014 Paris, France.

Corresponding author: Alicia Torriglia: alicia.torriglia@inserm.fr

Abstract

The wavelength-dependent impact of light has been mainly studied focusing on retina. In particular, an opposite effect of the two ends of the visible spectrum was observed, with blue wavelengths being harmful and red wavelengths being protective. However, few studies on the cornea indicate that the increasing exposition to artificial light due to digital devices is linked to an increase in computer vision syndrome affecting the cornea. In this study, we aim at deciphering the impact of blue and red LED light on a primary culture of corneal endothelial cells, by looking at cell death and proliferation, and at DNA replication and DNA breaks. Our results show that exposure to blue light at 5.35 J/cm²(455 nm) induces the inhibition of DNA replication and cell proliferation, and the formation of DNA breaks, highlighted by the formation of γH2AX foci and DNA fragmentation. Addition of red light at 0.3 J/cm² (630 nm) to blue light mitigates the formation of DNA damage and delays the kinetics of formation and repair of the damage. Interestingly, exposure of the corneal cells to red light alone induces the formation of γH2AX foci that do not correspond to DNA breaks, but to DNA replication forks in proliferative cells. Our results highlight the wavelength-dependent effect of light on the cornea, and point out that the formation of γH2AX foci is not always representative of DNA breaks. This emphasizes the importance of light spectrum in eye health, an important issue in today's changing light environment.

Keywords: cornea, phototoxicity, light, proliferation, DNA damage

1. Introduction

Despite being necessary for the vision, excessive exposure to light can be detrimental. Nowadays, the exposure of the population to artificial light, mostly digital devices composed of light emitting diodes (LED), is growing. Such LED devices emit a light with a high proportion of blue wavelengths, and few red wavelengths[1]. The wavelength-dependency of light-induced damage has mainly been evaluated on the retina, where exposure to blue light induces photoreceptor cell death while red light does not affect retinal cell viability [2,3].

The induction of DNA damage is one of the mechanisms involved in the decrease of cell viability, by altering DNA replication [4,5], and by promoting cell death [6,7]. Several forms of DNA damage have been characterized: structural changes affecting stability, oxidative damage to nucleotides, single-strand breaks and double-strand breaks (DSB). DNA damage occurs continuously in every cells and its accumulation overtime participates to cellular ageing or oncogenesis [8]. Visible light has been shown to damage DNA in several eye tissues in a wavelength-dependent manner[9,10]. Previous results on retinal pigment epithelial (RPE) cells have shown that blue and red light have a wavelength-dependent effect on the DNA damage formation and repair mechanism [11].

The cornea is the first component of the eye receiving the incident light. It is a structure composed of three layers: an epithelium that lays on a basal membrane (the Bowman's membrane), a stroma that represents 90% of the cornea, and an endothelium that lays on another basal membrane, the Descemet's membrane[12]. As a result of the increasing exposure to artificial light, more than 50% of the regular digital device users suffer from the so-called computer vision syndrome (CVS). CVS manifests itself as ocular irritation, burning, and dry eye syndrome, thus affecting the ocular surface and the cornea [13,14]. The study of the effect of visible light on the cornea has pointed out a wavelength-dependent response of the corneal tissue, with blue, green and red light affecting differently the properties of the bilayer membrane of the corneal tissue, as shown on total corneal extracts [15]. Moreover, the phototoxicity of ultra-violet (UV) wavelengths on the cornea has been extensively studied [16,17], and UV irradiation has been shown to induce DNA damage, and more particularly cyclobutane pyrimidine dimers [18].

Unlike previous studies that focused on UV exposure, this study focuses on visible light. Furthermore, its main aim is to decipher the effect of the two extremities of the visible spectrum (blue and red wavelengths). This was done on a primary culture of corneal endothelial cells, by looking at the cell viability and the induction of DNA breaks. The effect of the exposure to blue and red light are analyzed separately and following a simultaneous exposure, to investigate the importance of the spectral composition of the light on corneal cells.

2. Material & Methods

2.1. Cell culture

Bovine corneal endothelial (BCE) cells were a primary culture of corneal endothelial cells obtained from fresh cow eyes as described in Chifflet et al. [19]. BCE cells were cultured at 37°C, 5% CO_2, on 12-well plates with (for immunostaining) or without (for Comet Assay) glass coverslips. For experiments proposes the cells were seeded at 130 000 cells/cm². Cells were grown in MEM medium (Gibco™ 10370-047) supplemented with 10% fetal bovine serum (FBS), 0.5% penicillin/ streptomycin/ fungizone and 5 ng/mL Fibroblast Growth Factor, for two weeks to reach 100% confluence. Treatment of cells with etoposide (ETP) was used as a positive control for the induction of DNA breaks (Figure S1). The culture medium was replaced by phenol red-free DMEM/F12 (Gibco™ 11039-

021) containing 100 µM ETP (Alexis Corporation 270-209-M100). Cells were incubated for 2 h, then rinsed with phosphate buffer saline (PBS) containing Ca^{2+} and Mg^{2+} before fixation with 4% paraformaldehyde (PFA) for 10 min. To study proliferation, cells were used at passage 3. To study DNA damage on non-proliferative cells, cells were used at passage 7.

2.2. Light exposure

After replacing the culture medium with phenol red-free medium (DMEM/F12, Gibco™ 11039-021), BCE cells were exposed to LED light in an incubator with blue (455 nm, Joyland, D50SWD-B) and red (630 nm, Qasim, QA-SL0001-EU) LED strips on the top shelf at 46 cm over the cells. Cells were exposed for 2 h to blue light alone, red light alone, or blue and red lights simultaneously, then left in the dark in the incubator for 0 h, 1 h, 2 h, or 3 h. The light irradiance was 0.7 mW/cm² for blue light, 0.04 mW/cm² for red light and0.74 mW/cm² for blue+red light. This resulted in an exposure dose of 5.35 J/cm² (calculated as the radiant intensity in W/cm² multiplied by the time of exposure in seconds) for blue light, 0.3 J/cm² for red light and 5.65 J/cm² for blue+red lights (ratio blue/red 0.05, equivalent to a white LED 8000K). Cells not exposed to light were left in the dark in the incubator after medium replacement. The temperature of the incubator was monitored and maintained at 37°C throughout the light exposure to avoid any potential thermal effect of the exposure.

Images of the irradiated cells are provided as Figure S2.

2.3. Immunostaining

Cells grown on coverslips and exposed to light or ETP were rinsed in PBS containing Ca^{2+} and Mg^{2+} before fixation with 4% paraformaldehyde (PFA) for 10 min. The coverslips were then rinsed with PBS and stored at 4°C before immunostaining that was made within a week. For immunostaining, cells on coverslips were permeabilized with 0.3% Triton X-100 for 15 min at room temperature, then rinsed with PBS. They were incubated with the primary antibody (anti-γH2AX Ser139, Millipore 05-636, 1: 500; anti-Ki67, NovusBio NB500-170, 1: 100) in PBS with 1% Bovine Serum Albumin (BSA) for 1 h at room temperature. The coverslips were incubated for 1 h with the fluorophore-coupled secondary antibody (1: 200 in PBS with 1% BSA). Finally, they were incubated for 5 min with DAPI (4',6 diamidino-2-phenylindole) (1: 1000 in PBS), then mounted on slides with Fluoromount (Sigma, F4680-25ML).

2.4. EdU staining

To perform EdU staining of the BCE cells, we used the Click-iT™ Plus EdU Cell Proliferation Kit for Imaging, Alexa Fluor™ 488 dye (Invitrogen, C10637). 10 µM of EdU was added to the culture medium 15 min before cell fixation with 4% PFA for 10 min. Coverslips were then permeabilized with 0.3% Triton X-100 for 15 min at room temperature, then rinsed with PBS followed by 2 rinses with PBS+ 3% BSA. Coverslips were incubated for 30 min with the Click-iT® Plus reaction cocktail following manufacturer protocol. Then they were rinsed with with PBS+ 3% BSA and PBS before continuing with the primary antibody for the immunostaining as described above.

2.5. Comet Assay

The Comet Assay protocol was adapted from Olive and Banáth[20]. Briefly, glass slides were coated with 1% low melting point agarose (Invitrogen, 15517-014) in dH_2O. BCE cells were detached with Trypsin-EDTA 0.25% (Gibco™, 25200-056), retrieved in culture medium, centrifugated 5 min at 1,000 rpm and then resuspended in cold PBS. Cell density was adjusted to 8.10^4 cells/mL with PBS, then 0.1 mL of cell solution was added to 1 mL of 1% agarose at 40°C and laid on the agarose-coated slide. After gelling of the agarose for 2 min, an alkaline lysis was performed overnight at 4°C (1.2 M NaCl,

100 mM Na_2EDTA, 0.1% sodium lauryl sarcosinate, adjust pH at 10 with NaOH 1 M). Slides were immersed in TAE 1X solution (Gibco™, 15558-042) for 20 min before eletrophoresis for 40 min at 0.6 V/cm. Slides were rinsed in dH_2O and then stained with 2.5 µg/mL propidium iodure (Sigma, P4864-10ML) for 20 min before final rinse with dH_2O. Comets were imaged using the 20x objective of the fluorescent microscope Olympus BX51.

2.6. Image analysis

Images were obtained using a fluorescent microscope (Olympus BX51) with 4x, 20x, and oil immersion 40x objectives. All images were analyzed with the ImageJ software. For proliferative cells (in Figure 2), quantification of the number of γH2AX foci was done using the “Find Maxima” tool. For non-proliferative cells (in Figure 4), analysis of γH2AX foci was performed using the "Speckle Inspector" tool, which enables to only take into account foci located in a cell nucleus and to obtain the number and the size of the foci. Briefly, γH2AX and DAPI labeling images were binarized and used in "Speckle Inspector" as secondary objects for γH2AX and primary objects for DAPI. The following settings were used: primary objects (nuclei) must have a minimum size of 1000 px, and secondary objects (γH2AX foci) must be between 1 and 1000 px. Objects on the edges of the image were excluded. Analysis of the comet assay images was done using the "OpenComet" plugin [21] to obtain the Comet Tail Length and the Tail Moment. Counting of the apoptotic nuclei was done manually on 5 images per coverslips taken with the 20x objective. Countings of the DAPI-, EdU- and Ki67-stained cells were done on the images taken with the 4x objective (1 image per coverslip), using the "Find Maxima" tool. The number of apoptotic nuclei, EdU- or Ki67-positive cells was divided by the total number of DAPI nuclei.

2.7. Statistical analysis

All statistical analyses were performed with the GraphPad Prism software. We used the non-parametric Kruskal-Wallis test followed by Dunn’s post-tests. Results are expressed as Median (Interquartile Range – IQR); NE, B, B+R and R correspond to non-exposed, blue light-exposed, blue+red lights-exposed and red light-exposed cells, respectively. Statistical analyses are shown on tables 1 to 8.

3. Results

3.1. Wavelength-dependent impact of light exposure on cell death and proliferation

The effect of the exposure to light on corneal cells was first observed on cell viability. DAPI staining of the cells highlighted the presence of numerous apoptotic nuclei that seemed to be more frequent for blue and blue+red exposed cells (Figure 1A). Quantification of the proportion of apoptotic nuclei showed an increase for blue and blue+red lights that was significant only for blue+red lights at 2 hours (3.124 (IQR= 1.744) % apoptotic nuclei for non-exposed (NE) cells, 4.823 (IQR= 0.27) for blue (B) at 3 h, and 4.963 (IQR= 0.696) for blue+red (B+R) at 2h) (Figure 1B, statistical analysis on Table 1). We used anti-Ki67 staining as a proliferation marker and clearly observed an immediate inhibition of cell proliferation that persisted 4h after exposure to blue light, and which was not restoredby the addition of red light (12.63 (IQR= 2.55) % Ki67-positive cells for NE, 0.006653 (IQR= 0.01369) and 0.01911 (IQR= 0.02903) for B at 0 and 3h, 0.00 (IQR= 0.0136) and 0.00 (IQR= 0.00) for B+R at 0 and 3h) (Figure 1A, 1C, statistical analysis on Table 2). On the other hand, exposure to red light showed no impact on cell death or proliferation (3.519 (IQR= 0.207) % apoptotic nuclei and 8.848 (IQR= 3.175) % Ki67-positive cells for red (R) at 3 h).

		A											
	vs.	NE	B +0h	B +1h	B +2h	B +3h	B+R +0h	B+R +1h	B+R +2h	B+R +3h	R +0h	R +1h	R +2h	R +3h
	NE		ns	ns	ns	ns	ns	ns	*	ns	ns	ns	ns	ns
	B +0h			ns	ns	**	ns	ns	**	*	ns	ns	*	ns
	B +1h				ns	*	ns	ns	**	ns	ns	ns	ns	ns
	B +2h					ns	ns	ns	ns	ns	ns	ns	ns	ns
	B +3h						*	ns	ns	ns	*	ns	ns	ns
B	B+R +0h							ns	**	*	ns	ns	*	ns
	B+R +1h								ns	ns	ns	ns	ns	ns
	B+R +2h									ns	**	*	ns	ns
	B+R +3h										ns	ns	ns	ns
	R +0h											ns	ns	ns
	R +1h												ns	ns
	R +2h													ns
	R +3h													
A (horizontal) vs B (vertical)			A>B								A<B			

159

160 **Table 1:** Statistical analysis of the percentage of apoptotic nuclei depending on the lighting condition (non-
161 exposed – NE, blue – B, blue+red – B+R, red – R) and the time after exposure. Kruskal-Wallis test followed by
162 Dunn's post-tests. H(13)= 22.80. n≥ 2 coverslips per condition. ns: non-significant, *p<0.05, **p<0.01. In yellow:
163 horizontal condition is superior to vertical condition. In grey: horizontal condition is inferior to vertical
164 condition.

		A											
	vs.	NE	B +0h	B +1h	B +2h	B +3h	B+R +0h	B+R +1h	B+R +2h	B+R +3h	R +0h	R +1h	R +2h	R +3h
	NE		**	**	*	*	**	*	**	***	ns	ns	ns	ns
	B +0h			ns	ns	ns	ns	ns	ns	ns	**	*	ns	ns
	B +1h				ns	ns	ns	ns	ns	ns	*	*	ns	ns
	B +2h					ns	ns	ns	ns	ns	*	ns	ns	ns
	B +3h						ns	ns	ns	ns	*	ns	ns	ns
B	B+R +0h							ns	ns	ns	**	*	*	ns
	B+R +1h								ns	ns	*	ns	ns	ns
	B+R +2h									ns	*	*	ns	ns
	B+R +3h										***	**	*	*
	R +0h											ns	ns	ns
	R +1h												ns	ns
	R +2h													ns
	R +3h													
A (horizontal) vs B (vertical)			A>B								A<B			

165

Table 2: Statistical analysis of the percentage of Ki67-positive cells depending on the lighting condition (non-exposed – NE, blue – B, blue+red – B+R, red – R) and the time after exposure. Kruskal-Wallis test followed by Dunn's post-tests. H(13)= 31.45. n= 3 coverslips per condition. ns: non-significant, *p<0.05, **p<0.01, ***p<0.001. In yellow: horizontal condition is superior to vertical condition. In grey: horizontal condition is inferior to vertical condition.

3.2. Wavelength-dependent impact of light exposure on DNA replication and damage

The above results showed an inhibition of cell proliferation by blue light, which could also translate into an alteration of DNA replication. To test this hypothesis, we studied the incorporation of EdU in BCE cells added 15 min before cell fixation. As a replication stress during the S-phase can lead to the collapse of replication forks resulting in DNA breaks [5], and the exposure to blue light has already been shown to induce DNA damage [22], we used the staining of γH2AX to detect the presence of DNA damage following light exposure. Phosphorylation of H2AX is an early event in the presence of DNA DSB and is thus used as a marker of DNA damage [23]. Note that the subsequent dephosphorylation of H2AX is a sign of DSB repair. Simultaneous EdU and γH2AX staining showed that for non-exposed cells and cells exposed to red light, numerous cells displayed an incorporation of EdU, showing ongoing DNA replication (Figure 2A). Interestingly, EdU-positive nuclei also contained a high number of γH2AX foci, with a spatial correlation between γH2AX and EdU foci. On the contrary, BCE cells exposed to blue or blue+red lights showed no DNA replication sites but displayed numerous γH2AX foci (see the complete kinetics in Figure S3). Quantification of the percentage of EdU-positive nuclei confirmed the inhibition of DNA replication by blue light (2.831 (IQR= 1.204) % EdU-positive cells for NE, 0.009568 (IQR= 0.008181) for B at 1 h, 0.006203 (IQR= 0.009775) for B+R at 1 h, 4.063 (IQR= 5.315) for R at 1 h) (Figure 2B, statistical analysis on Table 3). The counting of γH2AX foci highlighted the presence of a high number of DNA replication-related foci in red light-exposed cells, while the number of γH2AX foci induced by blue and blue+red lights is not significantly higher than in non-exposed cells (144.7 (IQR= 47.6) γH2AX foci for NE, 258 (IQR= 65.7) for B at 1 h, 171 (IQR= 52) for B+R at 1 h, 342.3 (IQR= 38) for R at 1 h) (Figure 2C, statistical analysis on Table 4).

	A													
B	vs.	NE	B +0h	B +1h	B +2h	B +3h	B+R +0h	B+R +1h	B+R +2h	B+R +3h	R +0h	R +1h	R +2h	R +3h
	NE		**	**	**	**	*	***	**	**	ns	ns	ns	ns
	B +0h			ns	ns	ns	ns	ns	ns	ns	***	**	**	**
	B +1h				ns	ns	ns	ns	ns	ns	**	**	**	*
	B +2h					ns	ns	ns	ns	ns	***	***	**	**
	B +3h						ns	ns	ns	ns	**	**	**	*
	B+R +0h							ns	ns	ns	**	**	**	*
	B+R +1h								ns	ns	****	***	***	**
	B+R +2h									ns	***	**	**	*
	B+R +3h										**	**	**	*
	R +0h											ns	ns	ns
	R +1h												ns	ns
	R +2h													ns

	R +3h
A (horizontal) vs B (vertical)	A>B / A<B

Table 3: Statistical analysis of the percentage of EdU-positive cells depending on the lighting condition (non-exposed – NE, blue – B, blue+red – B+R, red – R) and the time after exposure. Kruskal-Wallis test followed by Dunn's post-tests. H(13)= 57.02. n= 6 coverslips per condition. ns: non-significant, *p<0.05, **p<0.01, ***p<0.001, ****p<0.0001. In yellow: horizontal condition is superior to vertical condition. In grey: horizontal condition is inferior to vertical condition.

		A											
	vs.	NE	B +0h	B +1h	B +2h	B +3h	B+R +0h	B+R +1h	B+R +2h	B+R +3h	R +0h	R +1h	R +2h	R +3h
	NE		ns	ns	ns	ns	ns	ns	ns	ns	**	**	**	*
	B +0h			ns	ns	ns	ns	ns	ns	ns	ns	ns	ns	ns
	B +1h				ns	ns	ns	ns	ns	ns	ns	ns	ns	ns
	B +2h					ns	ns	ns	ns	ns	ns	ns	ns	ns
	B +3h						ns	ns	ns	ns	*	ns	*	ns
B	B+R +0h							ns	ns	ns	**	*	*	ns
	B+R +1h								ns	ns	**	*	**	ns
	B+R +2h									ns	**	**	**	*
	B+R +3h										**	*	*	ns
	R +0h											ns	ns	ns
	R +1h												ns	ns
	R +2h													ns
	R +3h													
A (horizontal) vs B (vertical)		A>B								A<B				

Table 4: Statistical analysis of the number of γH2AX foci depending on the lighting condition (non-exposed – NE, blue – B, blue+red – B+R, red – R) and the time after exposure. Kruskal-Wallis test followed by Dunn's post-tests. H(13)= 30.44. n= 3 coverslips per condition. ns: non-significant, *p<0.05, **p<0.01. In yellow: horizontal condition is superior to vertical condition. In grey: horizontal condition is inferior to vertical condition.

3.3. Correlation between γH2AX foci and DNA breaks depending on the wavelength

As several *in vivo* studies have shown the harmlessness of an exposure to red light[1,24], the presence of many γH2AX foci induced by red light was intriguing. Recent studies have shown that the presence γH2AX foci could be independent of the presence of DNA damage [25]. In order to decipher whether the observed γH2AX foci were actually corresponding to DNA breaks, we evaluated the DNA fragmentation. The results of the Comet Assay on cells exposed to light and fixed 1 and 3 h after exposure showed that both blue and blue+red lights triggered the formation of a visible comet tail while the comets of cells exposed to red light were more rounded (Figure 3A). These observations were confirmed by the analysis of the tail length and the tail moment. Evaluation of tail length showed that exposure to red light induced no significant DNA damage compared to non-exposed cells (11 (IQR= 22.25) px for NE, 19 (IQR= 17.5) and 10 (IQR= 14) for R at 1 and 3 h, respectively),

while blue light induced DNA damage at 1 h that decreased at 3 h (34 (IQR= 18.5) px and 25 (IQR= 16.5) for B at 1 and 3 h, respectively). Such damage was mitigated by the addition of red light at 1 h, results at 3 h being similar for blue and blue+red (22.5 (IQR= 18.75) px and 26.5 (IQR= 24.25) for B+R at 1 and 3 h, respectively) (Figure 3B, statistical analysis on Table 5). The analysis of the tail moment further supported this result (Figure 3C, statistical analysis on Table 6). This parameter, that takes into account the tail length and its DNA content, also indicated that the tail moment was not significantly different between NE and red exposed cells after 1 h of exposure (0.4411 (IQR= 2.8893) for NE, 1.183 (IQR= 1.7971) for R at 1 h) and was significantly decreased at 3 h after red light exposure (0.402 (IQR= 0.82137)). On the contrary blue light increased the tail moment (3.473 (IQR= 3.115) and 1.929 (IQR= 3.066) for B at 1 and 3 h, respectively). This parameter was also decreased by the addition of red light to blue light at 1 h (2.039 (IQR= 2.6398) and 2.378 (IQR= 2.9956) for B+R at 1 and 3 h, respectively). These results indicated that although the γH2AX foci observed after blue light exposure corresponded to DNA damage, this was not the case for red light exposure.

A difference in the kinetics of DNA damage formation and repair between the exposure to blue and blue+red lights was also visible. The tail length and the tail moment for blue light increased 1 h after exposure and decreased 3 h after exposure. On the contrary, the ones for blue+red lights exposure stayed higher than the control at 1 and 3 h (Figure 2B, 2C).

		A						
	vs.	NE	B +1h	B +3h	B+R +1h	B+R +3h	R +1h	R +3h
B	NE		****	****	****	****	ns	*
	B +1h			***	****	**	****	****
	B +3h				ns	ns	**	****
	B+R +1h					ns	*	****
	B+R +3h						**	****
	R +1h							***
	R +3h							
A (horizontal) vs B (vertical)			A>B			A<B		

Table 5: Statistical analysis of Tail Length depending on the lighting condition (non-exposed – NE, blue – B, blue+red – B+R, red – R) and the time after exposure. Kruskal-Wallis test followed by Dunn's post-tests. H(7)=136.8. n≥ 69 comets per condition. ns: non-significant, *p<0.05, ***p<0.001, ****p<0.0001. In yellow: horizontal condition is superior to vertical condition. In grey: horizontal condition is inferior to vertical condition.

		A						
	vs.	NE	B +1h	B +3h	B+R +1h	B+R +3h	R +1h	R +3h
B	NE		****	****	***	****	ns	**
	B +1h			**	****	**	****	****
	B +3h				ns	ns	***	****
	B+R +1h					ns	*	****
	B+R +3h						***	****
	R +1h							***
	R +3h							
A (horizontal) vs B (vertical)			A>B			A<B		

Table 6: Statistical analysis of Tail Moment depending on the lighting condition (non-exposed – NE, blue – B, blue+red – B+R, red – R) and the time after exposure. Kruskal-Wallis test followed by Dunn's post-tests. H(7)=141.0. n≥ 69 comets per condition. ns: non-significant, *p<0.05, **p<0.01, ***p<0.001, ****p<0.0001. In yellow: horizontal condition is superior to vertical condition. In grey: horizontal condition is inferior to vertical condition.

3.4. Light-induced γH2AX foci formation in non-proliferative cells

The previous results showed an effect of light on the formation of γH2AX foci on proliferative cells, highlighting that red light-induced γH2AX foci corresponded to replication sites and not to DNA breaks. On the contrary, γH2AX foci induced by blue light corresponded to DNA damage. *In vivo*, human corneal endothelial cells display a limited proliferative capacity [26], thus we used confluent BCE cells at passage 7 to ensure the absence of proliferation in our cell culture, as no DNA replication was observe from passage 6 (Figure S4). The number and size of γH2AX foci were analyzed, the number of γH2AX foci being proportional to the number of DSB, and bigger foci representing a coalescence of multiple foci into one repair hub [27,28].

Non-exposed cells displayed few γH2AX foci, whereas cells exposed to blue, blue+red, and red lights often had several foci in each nucleus (Figure 4A). The analysis of the number of foci per nucleus (Figure 4B, statistical analysis on Table 7) and the size of the foci (Figure 4C, statistical analysis on Table 8) revealed a different kinetics according to the wavelength of light used, as observed above with the Comet assay. Exposure to blue light induced the significant formation of γH2AX foci that peaked at 1 h after exposure (2 (IQR= 4) foci/nucleus for NE, 4 (IQR= 5) for B at 1 h) before becoming comparable to the non-exposed cells at 3 h (2 (IQR= 4) foci/nucleus for B at 3 h). The size of the foci induced by blue light was maximum after the end of the exposure (5 (IQR= 14) px for NE, 7 (IQR= 15) for B at 0 h), showing a rapid induction of DNA damage followed by its repair. Addition of red to blue light led to the formation of fewer γH2AX foci compared to exposure to blue light alone (3 (IQR=6), 4 (IQR=5) and 3 (IQR=5.75) foci/nucleus for B at 0, 1 and 2 h respectively, and 2 (IQR=4), 3 (IQR= 4) and 3 (IQR= 5) for B+R at 0, 1, and 2 h respectively). The peak of the number and size of the foci was also delayed, with a maximum 2 h and 1 h after exposure to blue+red lights, respectively (3 (IQR= 5) foci/nucleus at 2 h and 6 (IQR= 13) px at 1 h). Interestingly, exposure to red light triggered the appearance of numerous γH2AX foci in BCE cells that remained unchanged 3 h after exposure. The number of foci induced by red light was greater than the one in the other conditions (up to 6 (IQR=7) foci/nucleus). Moreover, the size of these γH2AX foci induced by red light was also bigger than the ones found in non-exposed cells (7 (IQR= 16) pix for R at 0 h, against 5 (IQR= 14) for NE) or the ones induced by the exposure to blue (7 (IQR= 15) px at 0 h) and blue+red lights (6 (IQR= 15) px at 0h) and their size did not decrease. This showed that red light-induced formation of γH2AX foci also happened in the absence of DNA replication.

		A											
	vs.	NE	B +0h	B +1h	B +2h	B +3h	B+R +0h	B+R +1h	B+R +2h	B+R +3h	R +0h	R +1h	R +2h	R +3h
B	NE		****	****	****	****	****	**	****	****	****	****	****	****
	B +0h			****	ns	****	****	****	**	****	****	****	****	****
	B +1h				****	****	****	****	****	****	****	****	****	****
	B +2h					****	****	****	***	****	****	****	****	****
	B +3h						ns	****	****	****	****	****	****	****
	B+R							****	****	****	****	****	****	****

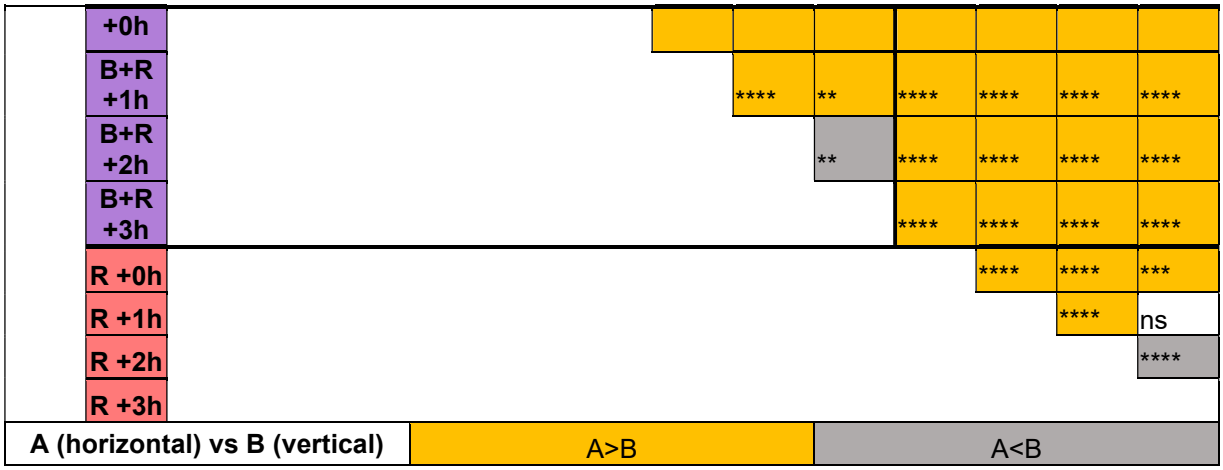

277

278 **Table 7:** Statistical analysis of the number of γH2AX foci per nucleus depending on the lighting condition (non-
279 exposed – NE, blue – B, blue+red – B+R, red – R) and the time after exposure. Kruskal-Wallis test followed by
280 Dunn's post-tests. H(13)=7413. n≥ 2892 analyzed cells per condition. ns: non-significant, **p<0.01,
281 ****p<0.0001. In yellow: horizontal condition is superior to vertical condition. In grey: horizontal condition is
282 inferior to vertical condition.

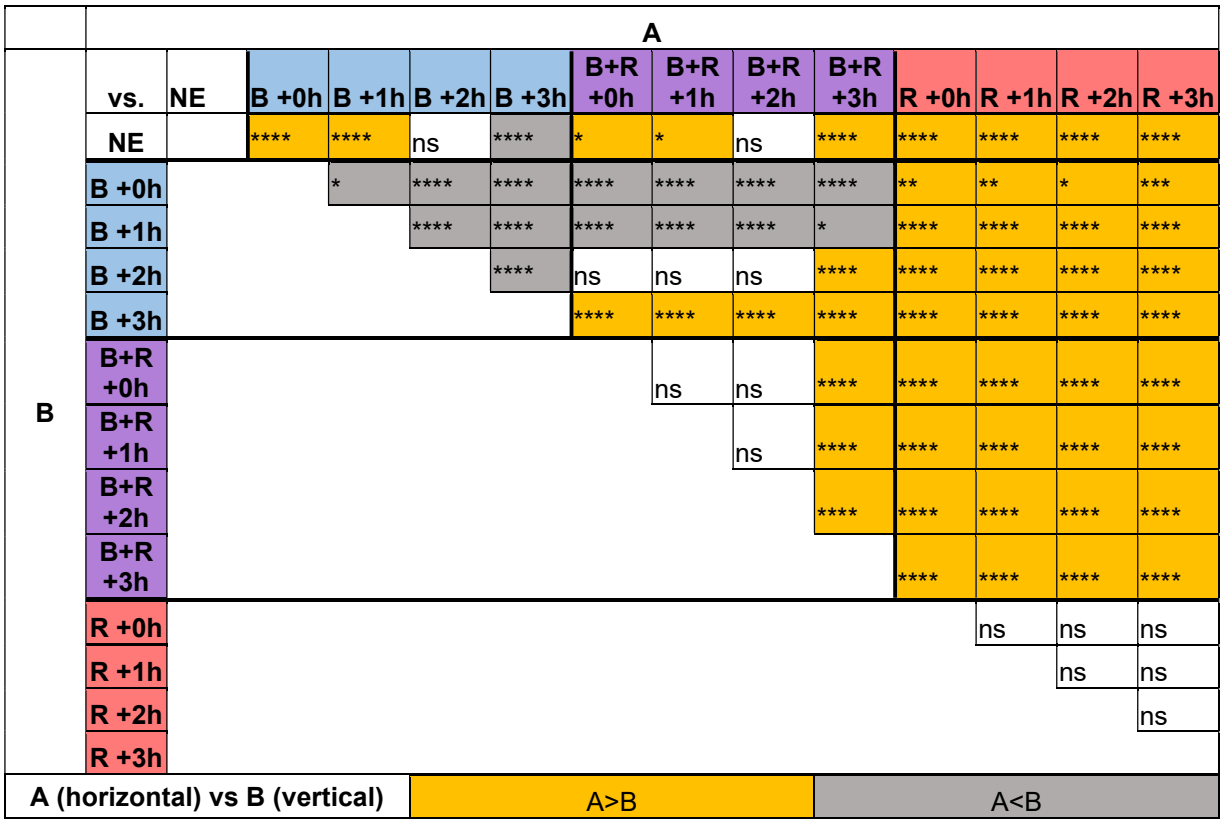

283

284 **Table 8:** Statistical analysis of the γH2AX area depending on the lighting condition (non-exposed – NE, blue – B,
285 blue+red – B+R, red – R) and the time after exposure. Kruskal-Wallis test followed by Dunn's post-tests.
286 H(13)=1414. n≥ 8311 analyzed foci per condition. ns: non-significant, *p<0.05, **p<0.01, ***p<0.001,
287 ****p<0.0001. In yellow: horizontal condition is superior to vertical condition. In grey: horizontal condition is
288 inferior to vertical condition.

289

4. Discussion

Our results show that exposure to blue light decreases cell viability by inhibiting cell proliferation, DNA replication and inducing DNA breaks. In our paradigm, the dose of red light is not sufficient to prevent the blue light-induced inhibition of the cell proliferation. Nevertheless, addition of red light to blue light mitigates the formation of DNA damage and delays the DNA damage formation and repair kinetic. We also show that exposure to red light alone induces the formation of numerous big and long lasting γH2AX foci that do not correspond to DNA breaks. In proliferative cells, these foci form at DNA replication sites, as red light does not affect the proliferation of the cells. These results indicate that lights of different wavelengths can have different biological effects on DNA damage, repair and replication,and highlight the importance of the spectral composition of the light that reaches exposed cells.

In this study, we use a primary cell culture of corneal cells. These cells are naturally daily exposed to light and display a limited genomic alteration compared to immortalized cell lines classically used for the study of DNA damage [29]. The four time points used to observe effect of light exposure (0-3 h after exposure to light) have been determined based on several papers studying the kinetic of γH2AX foci formation, which show that the number of γH2AX foci peaks in the first 3 h following the exposure to various stress (irradiation, X-rays, α-particles) [30–32] and notably UV-C where a first peak of γH2Ax foci is observed 1 h post exposure [33]. In our paradigm, the peak of γH2AX foci formation follows the exposure to blue and blue+red lights at 1 h and 2 h respectively, being coherent with the data found in the literature.

4.1. Blue light is deleterious for corneal cell viability

The inhibition of DNA replication and cell proliferation by the exposure to blue light is clearly showed here. Such a result is in accordance with other studies on corneal epithelial cells (HCE-2) in which an exposure to blue LED light (465–475 nm) slows down the rate of closure in a corneal wound healing model and increases cell death in a dose-dependent manner [34]. The observed effects induced by blue light *in vitro* on DNA and proliferation could also contribute to long term negative effect such as CVS. Indeed, it has been shown *in vivo* that chronic exposure to blue light (450 nm, 1,000 lx) 12 h a day for 28 days induces a negative impact on rat ocular surface, that could manifest as dry eye [35].

In the cornea, blue light (410 and 480 nm) has already been shown to induce the production of reactive oxygen species and to decrease the viability of corneal epithelial cells *in vitro* at doses superior to 5 J/cm² [36]. The capacity of blue light to induce DNA damage has also been previously observed *in vitro* in human keratinocytes (415 nm) [22], human retinal pigment epithelial cells (468 nm) [37], and a primary culture of rat retinal cells [10]. Thus, the induction of DNA damage, indicated by γH2AX foci formation and DNA fragmentation, following the exposure of the corneal endothelial cells to blue light is in accordance with already published results on various cell types.

It is to note that the observed effects of blue light on DNA damage induction and cell proliferation might be cell type-dependent and dose-dependent. Taoufik et al. have shown on human gingival fibroblasts exposed to blue LED at 162 J/cm² that blue light does not immediately inhibits DNA replication, and suggested that the inhibition of cell proliferation is not caused by DNA damage induction in these cells [38].

4.2. Red light does not induce DNA breaks

The role of red light is more complex. Without prior or simultaneous exposure to another stress (such as blue light), our results clearly show the formation of γH2AX foci. Similar results have been obtained from other research teams on fibroblasts [39] or retinal pigment epithelial cells [37]. These

authors suggested that red light induces DNA damage. However, our results from the Comet Assay and the study done by Wang et al. disagree with this point of view. Wang et al. conclude that exposure of human dermal fibroblasts cells to several doses of red light (633 nm at 320, 640, and 1280 J/cm²) does not induce the formation of DNA damage in the form of cyclobutane pyrimidine dimers or 6-4 photoproducts [40]. These results raise the question of the actual matching between the formation of γH2AX foci and the presence of DSB. It is to note that recent studies highlight the limits of the use of γH2AX staining as a marker of DSB [25,41]. The presence of γH2AX foci has also been associated with DNA distortion [42] and with replication stress in UV-treated S-phase cells [43], responses that are unrelated to the presence of DSB.

In replicative cells, the overlap between γH2AX foci and EdU staining observed after the exposure of BCE cells to red light is thus coherent with the formation of γH2AX foci at DNA replication forks. This is consistent with the fact that a replication stress during the S-phase can lead to the collapse of replication forks resulting in DNA breaks [5]. Red light-induced γH2AX foci could watch over DNA replication [44] by labelling stalled replication forks before DSB formation, and having the ability to promote replication forks stability, restart, and DSB repair if the fork collapses by enabling the gathering of DNA synthesis resources [45–47]. This highlights a potential protective mechanism triggered by the exposure to red light.

In vivo studies [2,24] and the repeated use of low-level red light therapy in myopic patients [48,49] point out the safety of the exposure to red light for the eye and notably the retina. In concordance with this, the formation of γH2AX foci observed in non-replicative BCE cells could correspond to a preventive activation of the DNA repair machinery.

4.3. Addition of red light to blue light partially protects from DNA damage

While exposure to blue light is detrimental for the cells, addition of red light mitigates the DNA damage in our results, by reducing the global amount of γH2AX foci in non-replicative cells. Hence, the immediate formation of γH2AX foci induced by red light could trigger the fast repair of the first blue-light induced DNA damage. A similar protective effect of red light on blue-light induced damage has been shown in corneal epithelial cells *in vitro* in which red light reduces blue-light-induced cell death [34]. The protective effect of red light is also widely used for skin wound healing in a process called photobiomodulation. Low level red or near infrared light therapy helps following UV-induced damage or burned skin through enhancement of DNA repair mechanisms [39,50,51] and through enhancement of cell proliferation [52]. Such action of red light on the DNA repair pathway is in accordance with our findings. Nevertheless, in our paradigm, the dose of red light is not sufficient to enhance cell proliferation or prevent light-induced cell death. It is to note that we use a dose of 0.3 J/cm² of red light, whereas a red light-induced enhancement of cell proliferation is observed in the literature at doses of 2.4 J/cm² on fibroblasts [53] and 3 J/cm² on human adipose-derived stem cells [54].

5. Conclusion

To conclude, the light effect on DNA damage and cell proliferation is wavelength-dependent. Both extremities of the visible spectrum show opposite effects, blue light being deleterious and red light being protective. This points out the importance of the spectral composition of the light in cell's effects and suggests that an enrichment in red wavelengths could be beneficial to prevent long-term light-induced damage. This is clearly seen in our study and is its major novelty, together with the effect of red light on DNA break and repair. The molecular mechanisms behind the effects seen after

exposure to red light need to be fully investigated, using longer kinetics, for instance. In addition, although other authors have shown that human corneal cells behave in the same way as the bovine cells used in this study [34], the findings described here should be investigated in cells of human origin and on *in vivo* models in order to use this study to assess the risk to the human cornea.

6. Acknowledgement

Authors thank Emilie Picard for providing the spectrophotometer device and the Ecole Nationale Vétérinaired'Alfort for the bovine eyes.

7. Author contributions

Anaïs Françon: Conceptualization, Investigation, Formal analysis, Visualization, Writing – Original Draft. **Francine Behar-Cohen:** Resources, Writing – Reviewing & Editing. **Alicia Torriglia:** Conceptualization, Supervision, Investigation, Writing – Reviewing & Editing, Funding acquisition.

8. Funding sources

This work was supported by ANSES (contrat 2022/EST/134).

9. References

[1] A. Françon, A. Torriglia, Cell death mechanisms in retinal phototoxicity, J. Photochem. Photobiol. 15 (2023) 100185. https://doi.org/10.1016/j.jpap.2023.100185.

[2] A. Françon, F. Behar-Cohen, A. Torriglia, The blue light hazard and its use on the evaluation of photochemical risk for domestic lighting. An *in vivo* study, Environ. Int. 184 (2024) 108471. https://doi.org/10.1016/j.envint.2024.108471.

[3] I. Jaadane, P. Boulenguez, S. Chahory, S. Carré, M. Savoldelli, L. Jonet, F. Behar-Cohen, C. Martinsons, A. Torriglia, Retinal damage induced by commercial light emitting diodes (LEDs), Free Radic. Biol. Med. 84 (2015) 373–384. https://doi.org/10.1016/j.freeradbiomed.2015.03.034.

[4] H.J. Edenberg, Inhibition of DNA replication by ultraviolet light, Biophys. J. 16 (1976) 849–860. https://doi.org/10.1016/S0006-3495(76)85735-9.

[5] S. Saxena, L. Zou, Hallmarks of DNA replication stress, Mol. Cell 82 (2022) 2298–2314. https://doi.org/10.1016/j.molcel.2022.05.004.

[6] E.A. Prokhorova, A.Y. Egorshina, B. Zhivotovsky, G.S. Kopeina, The DNA-damage response and nuclear events as regulators of nonapoptotic forms of cell death, Oncogene 39 (2020) 1–16. https://doi.org/10.1038/s41388-019-0980-6.

[7] W.P. Roos, A.D. Thomas, B. Kaina, DNA damage and the balance between survival and death in cancer biology, Nat. Rev. Cancer 16 (2016) 20–33. https://doi.org/10.1038/nrc.2015.2.

[8] B. Schumacher, J. Pothof, J. Vijg, J.H.J. Hoeijmakers, The central role of DNA damage in the ageing process, Nature 592 (2021) 695–703. https://doi.org/10.1038/s41586-021-03307-7.

[9] C. Xie, X. Li, J. Tong, Y. Gu, Y. Shen, Effects of white light-emitting diode (LED) light exposure with different Correlated Color Temperatures (CCTs) on human lens epithelial cells in culture, Photochem. Photobiol. 90 (2014) 853–859. https://doi.org/10.1111/php.12250.

[10] P. Chen, Z. Lai, Y. Wu, L. Xu, X. Cai, J. Qiu, P. Yang, M. Yang, P. Zhou, J. Zhuang, J. Ge, K. Yu, J. Zhuang, Retinal Neuron Is More Sensitive to Blue Light-Induced Damage than Glia Cell Due to DNA Double-Strand Breaks, Cells 8 (2019) 68. https://doi.org/10.3390/cells8010068.

[11] A. Françon, K. Delaunay, T. Jaworski, C. Lebon, E. Picard, J. Youale, F. Behar-Cohen, A. Torriglia, Phototoxicity of low doses of light and influence of the spectral composition on human RPE cells, Sci. Rep. 14 (2024) 6839. https://doi.org/10.1038/s41598-024-56980-9.
[12] A.O. Eghrari, S.A. Riazuddin, J.D. Gottsch, Chapter Two - Overview of the Cornea: Structure, Function, and Development, in: J.F. Hejtmancik, J.M. Nickerson (Eds.), Prog. Mol. Biol. Transl. Sci., Academic Press, 2015: pp. 7–23. https://doi.org/10.1016/bs.pmbts.2015.04.001.
[13] É. Auffret, G. Gomart, T. Bourcier, D. Gaucher, C. Speeg-Schatz, A. Sauer, [Digital eye strain. Symptoms, prevalence, pathophysiology, and management], J. Fr. Ophtalmol. 44 (2021) 1605–1610. https://doi.org/10.1016/j.jfo.2020.10.002.
[14] C. Blehm, S. Vishnu, A. Khattak, S. Mitra, R.W. Yee, Computer vision syndrome: a review, Surv. Ophthalmol. 50 (2005) 253–262. https://doi.org/10.1016/j.survophthal.2005.02.008.
[15] S.S. Mahmoud, I.H. Ibrahim, A.S.M. Sallam, G.W. Ali, Correction: Paradox response of cornea to different color intensities of visible light: An experimental study, PLoS ONE 14 (2019) e0212392. https://doi.org/10.1371/journal.pone.0212392.
[16] N.C. Delic, J.G. Lyons, N. Di Girolamo, G.M. Halliday, Damaging Effects of Ultraviolet Radiation on the Cornea, Photochem. Photobiol. 93 (2017) 920–929. https://doi.org/10.1111/php.12686.
[17] S. Kaidzu, K. Sugihara, M. Sasaki, A. Nishiaki, T. Igarashi, M. Tanito, Evaluation of acute corneal damage induced by 222-nm and 254-nm ultraviolet light in Sprague-Dawley rats, Free Radic. Res. 53 (2019) 611–617. https://doi.org/10.1080/10715762.2019.1603378.
[18] T. Volatier, B. Schumacher, C. Cursiefen, M. Notara, UV Protection in the Cornea: Failure and Rescue, Biology 11 (2022) 278. https://doi.org/10.3390/biology11020278.
[19] S. Chifflet, J.A. Hernández, S. Grasso, A. Cirillo, Nonspecific depolarization of the plasma membrane potential induces cytoskeletal modifications of bovine corneal endothelial cells in culture, Exp. Cell Res. 282 (2003) 1–13.
[20] P.L. Olive, J.P. Banáth, The comet assay: a method to measure DNA damage in individual cells, Nat. Protoc. 1 (2006) 23–29. https://doi.org/10.1038/nprot.2006.5.
[21] B.M. Gyori, G. Venkatachalam, P.S. Thiagarajan, D. Hsu, M.-V. Clement, OpenComet: An automated tool for comet assay image analysis, Redox Biol. 2 (2014) 457–465. https://doi.org/10.1016/j.redox.2013.12.020.
[22] C. Chamayou-Robert, C. DiGiorgio, O. Brack, O. Doucet, Blue light induces DNA damage in normal human skin keratinocytes, Photodermatol. Photoimmunol. Photomed. 38 (2022) 69–75. https://doi.org/10.1111/phpp.12718.
[23] L.J. Kuo, L.-X. Yang, Gamma-H2AX - a novel biomarker for DNA double-strand breaks, Vivo Athens Greece 22 (2008) 305–309.
[24] A. Françon, L. Jonet, F. Behar-Cohen, A. Torriglia, Repeated exposure to low doses of light induces retinal damage *in vivo* in a wavelength-dependent manner, Ecotoxicol. Environ. Saf. 290 (2025) 117605. https://doi.org/10.1016/j.ecoenv.2024.117605.
[25] K. Solarczyk, M. Kordon-Kiszala, Let's not take DNA breaks for granted. The importance of direct detection of DNA breaks for the successful development of DDR inhibitors, Front. Cell Dev. Biol. 11 (2023). https://www.frontiersin.org/articles/10.3389/fcell.2023.1118716 (accessed February 22, 2024).
[26] J. Chen, Z. Li, L. Zhang, S. Ou, Y. Wang, X. He, D. Zou, C. Jia, Q. Hu, S. Yang, X. Li, J. Li, J. Wang, H. Sun, Y. Chen, Y.-T. Zhu, S.C.G. Tseng, Z. Liu, W. Li, Descemet's Membrane Supports Corneal Endothelial Cell Regeneration in Rabbits, Sci. Rep. 7 (2017) 6983. https://doi.org/10.1038/s41598-017-07557-2.
[27] R. Bermejo, A. Kumar, M. Foiani, Preserving the genome by regulating chromatin association with the nuclear envelope, Trends Cell Biol. 22 (2012) 465–473. https://doi.org/10.1016/j.tcb.2012.05.007.
[28] T. Neumaier, J. Swenson, C. Pham, A. Polyzos, A.T. Lo, P. Yang, J. Dyball, A. Asaithamby, D.J. Chen, M.J. Bissell, S. Thalhammer, S.V. Costes, Evidence for formation of DNA repair centers and dose-response nonlinearity in human cells, Proc. Natl. Acad. Sci. 109 (2012) 443–448. https://doi.org/10.1073/pnas.1117849108.

[29] K. Iemura, H. Anzawa, R. Funayama, R. Iwakami, K. Nakayama, K. Kinoshita, K. Tanaka, High levels of chromosomal instability facilitate the tumor growth and sphere formation, Cancer Sci. 113 (2022) 2727–2737. https://doi.org/10.1111/cas.15457.
[30] N.T. Martin, S.A. Nahas, R. Tunuguntla, F. Fike, R.A. Gatti, Assessing "radiosensitivity" with kinetic profiles of γ-H2AX, 53BP1 and BRCA1 foci, Radiother. Oncol. J. Eur. Soc. Ther. Radiol. Oncol. 101 (2011) 35–38. https://doi.org/10.1016/j.radonc.2011.05.065.
[31] M. Ricoul, T.S. Gnana Sekaran, P. Brochard, C. Herate, L. Sabatier, γ-H2AX Foci Persistence at Chromosome Break Suggests Slow and Faithful Repair Phases Restoring Chromosome Integrity, Cancers 11 (2019) E1397. https://doi.org/10.3390/cancers11091397.
[32] E. Staaf, K. Brehwens, S. Haghdoost, J. Czub, A. Wojcik, Gamma-H2AX foci in cells exposed to a mixed beam of X-rays and alpha particles, Genome Integr. 3 (2012) 8. https://doi.org/10.1186/2041-9414-3-8.
[33] O. Staszewski, T. Nikolova, B. Kaina, Kinetics of γ-H2AX focus formation upon treatment of cells with UV light and alkylating agents, Environ. Mol. Mutagen. 49 (2008) 734–740. https://doi.org/10.1002/em.20430.
[34] C. Núñez-Álvarez, N.N. Osborne, Enhancement of corneal epithelium cell survival, proliferation and migration by red light: Relevance to corneal wound healing, Exp. Eye Res. 180 (2019) 231–241. https://doi.org/10.1016/j.exer.2019.01.003.
[35] L. Nan, Y. Zhang, H. Song, Y. Ye, Z. Jiang, S. Zhao, Influence of Light-EmittingDiode-Derived Blue Light Overexposure on Rat Ocular Surface, J. Ophthalmol. 2023 (2023) 1097704. https://doi.org/10.1155/2023/1097704.
[36] J.-B. Lee, S.-H. Kim, S.-C. Lee, H.-G. Kim, H.-G. Ahn, Z. Li, K.C. Yoon, Blue light-induced oxidative stress in human corneal epithelial cells: protective effects of ethanol extracts of various medicinal plant mixtures, Invest. Ophthalmol. Vis. Sci. 55 (2014) 4119–4127. https://doi.org/10.1167/iovs.13-13441.
[37] E. Chamorro, C. Bonnin-Arias, M.J. Pérez-Carrasco, J.M. de Luna, D. Vázquez, C. Sánchez-Ramos, Effects of Light-emitting Diode Radiations on Human Retinal Pigment Epithelial Cells *In Vitro*, Photochem. Photobiol. 89 (2013) 468–473. https://doi.org/10.1111/j.1751-1097.2012.01237.x.
[38] K. Taoufik, E. Mavrogonatou, T. Eliades, L. Papagiannoulis, G. Eliades, D. Kletsas, Effect of blue light on the proliferation of human gingival fibroblasts, Dent. Mater. Off. Publ. Acad. Dent. Mater. 24 (2008) 895–900. https://doi.org/10.1016/j.dental.2007.10.006.
[39] Y.J. Kim, H.-J. Kim, H.L. Kim, H.J. Kim, H.S. Kim, T.R. Lee, D.W. Shin, Y.R. Seo, A Protective Mechanism of Visible Red Light in Normal Human Dermal Fibroblasts: Enhancement of GADD45A-Mediated DNA Repair Activity, J. Invest. Dermatol. 137 (2017) 466–474. https://doi.org/10.1016/j.jid.2016.07.041.
[40] J.Y. Wang, E. Austin, J. Jagdeo, Visible red light does not induce DNA damage in human dermal fibroblasts, J. Biophotonics 15 (2022) e202200023. https://doi.org/10.1002/jbio.202200023.
[41] J.E. Cleaver, L. Feeney, I. Revet, Phosphorylated H2Ax is not an unambiguous marker for DNA double-strand breaks, Cell Cycle 10 (2011) 3223–3224. https://doi.org/10.4161/cc.10.19.17448.
[42] P. Rybak, A. Hoang, L. Bujnowicz, T. Bernas, K. Berniak, M. Zarębski, Z. Darzynkiewicz, J. Dobrucki, Low level phosphorylation of histone H2AX on serine 139 (γH2AX) is not associated with DNA double-strand breaks, Oncotarget 7 (2016) 49574–49587. https://doi.org/10.18632/oncotarget.10411.
[43] S. Dhuppar, S. Roy, A. Mazumder, γH2AX in the S Phase after UV Irradiation Corresponds to DNA Replication and Does Not Report on the Extent of DNA Damage, Mol. Cell. Biol. 40 (2020) e00328-20. https://doi.org/10.1128/MCB.00328-20.
[44] W.-Z. Tu, B. Li, B. Huang, Y. Wang, X.-D. Liu, H. Guan, S.-M. Zhang, Y. Tang, W.-Q. Rang, P.-K. Zhou, γH2AX foci formation in the absence of DNA damage: mitotic H2AX phosphorylation is mediated by the DNA-PKcs/CHK2 pathway, FEBS Lett. 587 (2013) 3437–3443. https://doi.org/10.1016/j.febslet.2013.08.028.

[45] R.A. Chanoux, B. Yin, K.A. Urtishak, A. Asare, C.H. Bassing, E.J. Brown, ATR and H2AX Cooperate in Maintaining Genome Stability under Replication Stress *, J. Biol. Chem. 284 (2009) 5994–6003. https://doi.org/10.1074/jbc.M806739200.
[46] C.-L. Hsu, S.Y. Chong, C.-Y. Lin, C.-F. Kao, Histone dynamics during DNA replication stress, J. Biomed. Sci. 28 (2021) 48. https://doi.org/10.1186/s12929-021-00743-5.
[47] B.M. Sirbu, F.B. Couch, J.T. Feigerle, S. Bhaskara, S.W. Hiebert, D. Cortez, Analysis of protein dynamics at active, stalled, and collapsed replication forks, Genes Dev. 25 (2011) 1320–1327. https://doi.org/10.1101/gad.2053211.
[48] G. Liu, B. Li, H. Rong, B. Du, B. Wang, J. Hu, B. Zhang, R. Wei, Axial Length Shortening and Choroid Thickening in Myopic Adults Treated with Repeated Low-Level Red Light, J. Clin. Med. 11 (2022) 7498. https://doi.org/10.3390/jcm11247498.
[49] R. Xiong, Z. Zhu, Y. Jiang, W. Wang, J. Zhang, Y. Chen, G. Bulloch, Y. Yuan, S. Zhang, M. Xuan, J. Zeng, M. He, Longitudinal Changes and Predictive Value of Choroidal Thickness for Myopia Control after Repeated Low-Level Red-Light Therapy, Ophthalmology 0 (2022). https://doi.org/10.1016/j.ophtha.2022.10.002.
[50] L.P.S. Sergio, V.M.A. Campos, S.C. Vicentini, A.L. Mencalha, F. de Paoli, A.S. Fonseca, Low-intensity red and infrared lasers affect mRNA expression of DNA nucleotide excision repair in skin and muscle tissue, Lasers Med. Sci. 31 (2016) 429–435. https://doi.org/10.1007/s10103-016-1870-6.
[51] E.T.L. Trajano, A.L. Mencalha, A. Monte-Alto-Costa, L.C. Pôrto, A. de Souza da Fonseca, Expression of DNA repair genes in burned skin exposed to low-level red laser, Lasers Med. Sci. 29 (2014) 1953–1957. https://doi.org/10.1007/s10103-014-1612-6.
[52] Y. Umino, M. Denda, Effect of red light on epidermal proliferation and mitochondrial activity, Skin Res. Technol. 29 (2023) e13447. https://doi.org/10.1111/srt.13447.
[53] P.L.V. Lima, C.V. Pereira, N. Nissanka, T. Arguello, G. Gavini, C.M. da C. Maranduba, F. Diaz, C.T. Moraes, Photobiomodulation enhancement of cell proliferation at 660 nm does not require cytochrome *c* oxidase, J. Photochem. Photobiol. B 194 (2019) 71–75. https://doi.org/10.1016/j.jphotobiol.2019.03.015.
[54] Y. Wang, Y.-Y. Huang, Y. Wang, P. Lyu, M.R. Hamblin, Red (660 nm) or near-infrared (810 nm) photobiomodulation stimulates, while blue (415 nm), green (540 nm) light inhibits proliferation in human adipose-derived stem cells, Sci. Rep. 7 (2017) 7781. https://doi.org/10.1038/s41598-017-07525-w.

Figure captions

Figure 1: Effect of the exposure to light on cell death and cell proliferation. A. Staining of proliferative cells using anti-Ki67 antibody (red) and DAPI (blue) in BCE cells exposed to blue (B), blue+red (B+R) or red (R) lights, or non-exposed (NE), and fixed at different time following light exposure: 0, 1, 2 and 3 hours. Arrows indicate apoptotic nuclei. Scale bar= 20 µm. B. Quantification of the proportion of apoptotic nuclei depending on the lighting condition and the time after exposure. n≥ 2 coverslips per condition. C. Quantification of the proportion of Ki67-positive cells depending on the lighting condition and the time after exposure. The number of apoptotic nuclei and Ki67-positive cells was divided by the total number of counted nuclei. n= 3 coverslips per condition. Graphs represent the median with the interquartile range. Statistical analysis of the graphs is shown in Table 1 and 2.

Figure 2: Correlation between replicative foci and γH2AX foci depending on the light exposure. A. Anti-γH2AX (red), EdU (green) and DAPI (blue) staining of BCE cells exposed to blue (B), blue+red (B+R) or red (R) lights, or non-exposed (NE), and fixed at 1h after light exposure. EdU was added to the culture medium 15 min before cell fixation. Scale bar= 20 µm.B. Quantification of the proportion of EdU-stained cells depending on the lighting condition and the time after exposure. The number of EdU-stained cells was divided by the total number of counted nuclei. n= 6 coverslips per condition. C. Quantification of number of γH2AX foci depending on the lighting condition and the time after exposure. n= 3 coverslips per condition. Graphs represent the median with the interquartile range. Statistical analysis of the graphs is shown in Table 3 and 4.

Figure 3: Comet Assay on cells exposed to light. A. Representative comets of BCE cells exposed to blue (B), blue+red (B+R) or red (R) lights, or non-exposed (NE), and fixed at 1h and 3h after light exposure. Scale bar= 20 µm. B. Distribution of Comet Tail Length depending on the lighting condition and the time after exposure. n≥ 69 comets per condition. C. Distribution of Tail Moment (Tail length times Tail DNA %) depending on the lighting condition and the time after exposure. n≥ 69 comets per condition. Violin plots show the median (red line) and the quartiles (dotted lines). Statistical analysis of the graphs is shown in Table 5 and 6.

Figure 4: Effect of the exposure to light on the presence of DNA damage foci in cells. A. Staining of DNA damage using anti-γH2AX antibody (red) and DAPI (blue) in BCE cells exposed to blue (B), blue+red (B+R) or red (R) lights, or non-exposed (NE), and fixed at different time following light exposure: 0, 1, 2 and 3 hours. Scale bar= 20 µm. B. Distribution of the number of γH2AX foci per nucleus depending on the lighting condition and the time after exposure. n≥ 2892 analyzed cells per condition. C. Distribution of the size of the γH2AX foci depending on the lighting condition and the time after exposure. n≥ 8311 analyzed foci per condition. Violin plots show the median (red line) and the quartiles (dotted lines). Statistical analysis of the graphs is shown in Table 7 and 8.

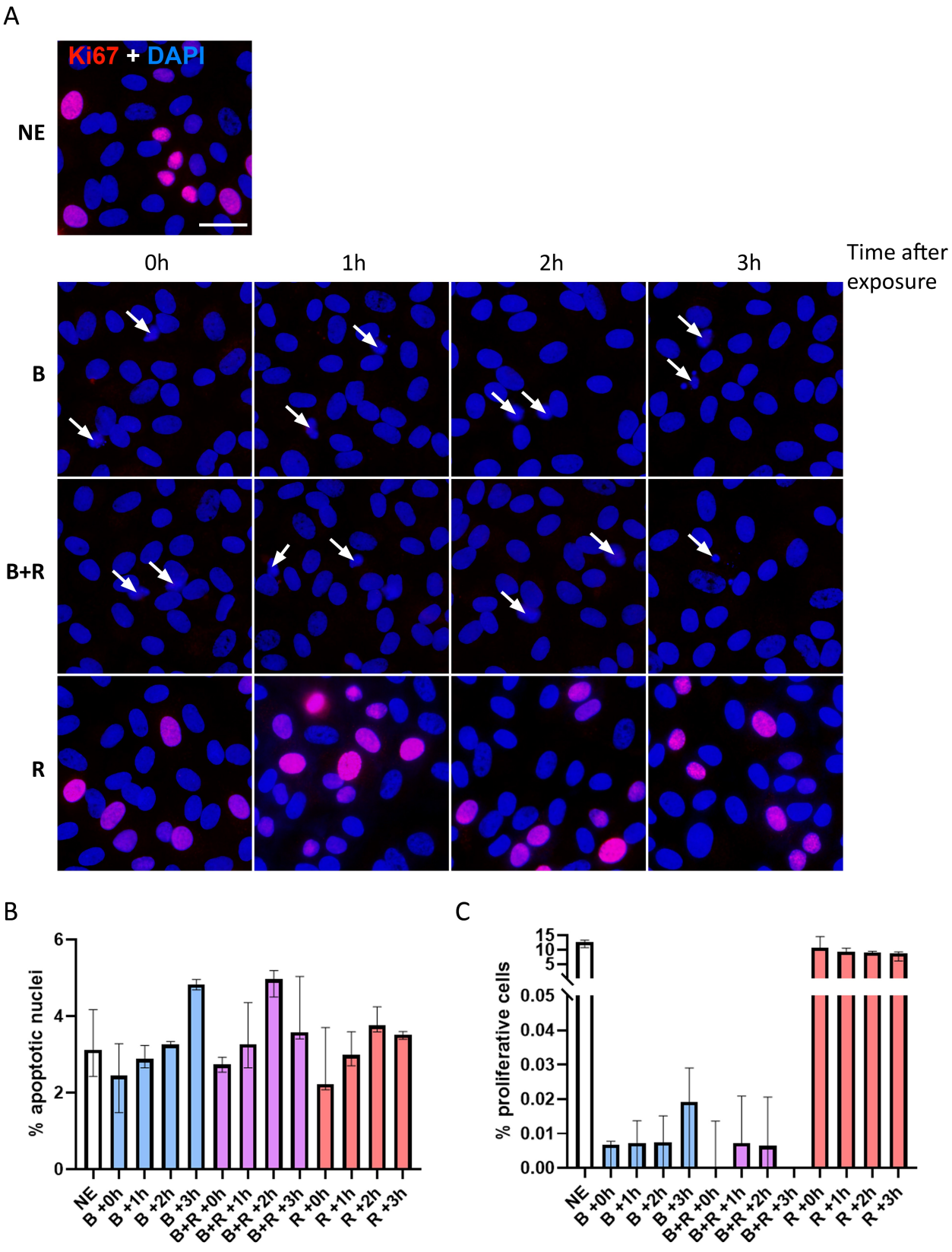
A
Ki67 + DAPI
NE
0h
1h
2h
3h
Time after exposure
B
B+R
R
B
% apoptotic nuclei
0
2
4
6
NE
B +0h
B +1h
B +2h
B +3h
B+R +0h
B+R +1h
B+R +2h
B+R +3h
R +0h
R +1h
R +2h
R +3h
C
% proliferative cells
0.00
0.01
0.02
0.03
0.04
0.05
5
10
15

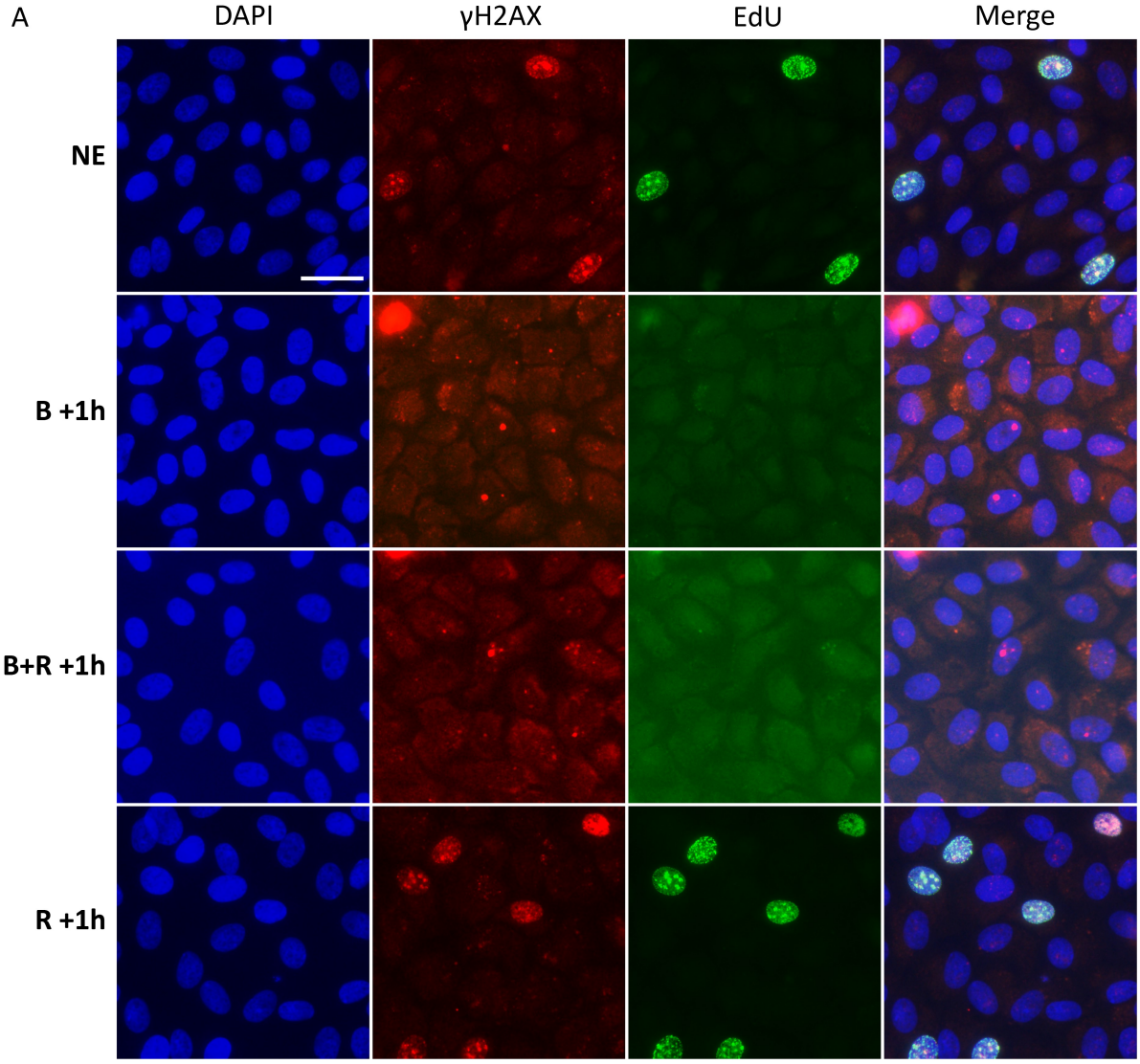
A
DAPI
γH2AX
EdU
Merge
NE
B +1h
B+R +1h
R +1h

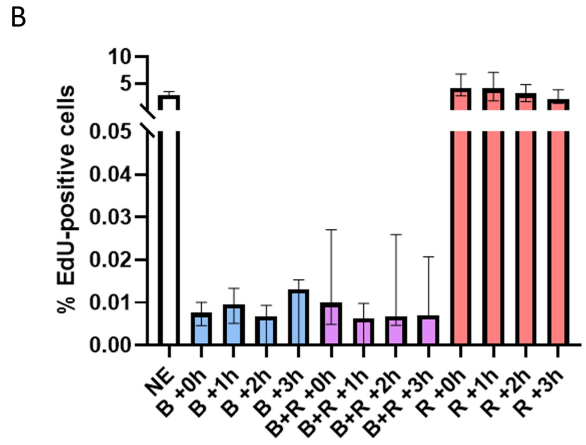
B
% EdU-positive cells
10
5
0.05
0.04
0.03
0.02
0.01
0.00
NE
B +0h
B +1h
B +2h
B +3h
B+R +0h
B+R +1h
B+R +2h
B+R +3h
R +0h
R +1h
R +2h
R +3h

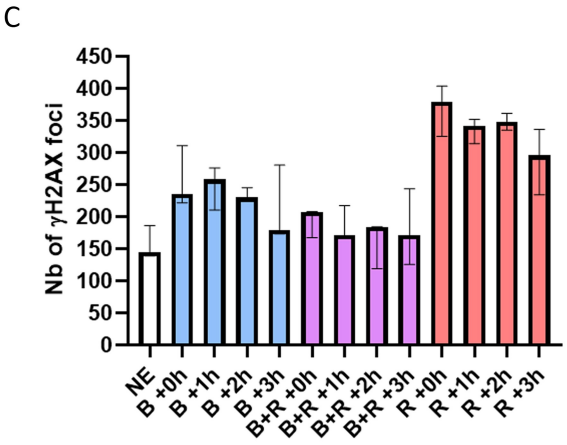
C
Nb of γH2AX foci
450
400
350
300
250
200
150
100
50
0
NE
B +0h
B +1h
B +2h
B +3h
B+R +0h
B+R +1h
B+R +2h
B+R +3h
R +0h
R +1h
R +2h
R +3h

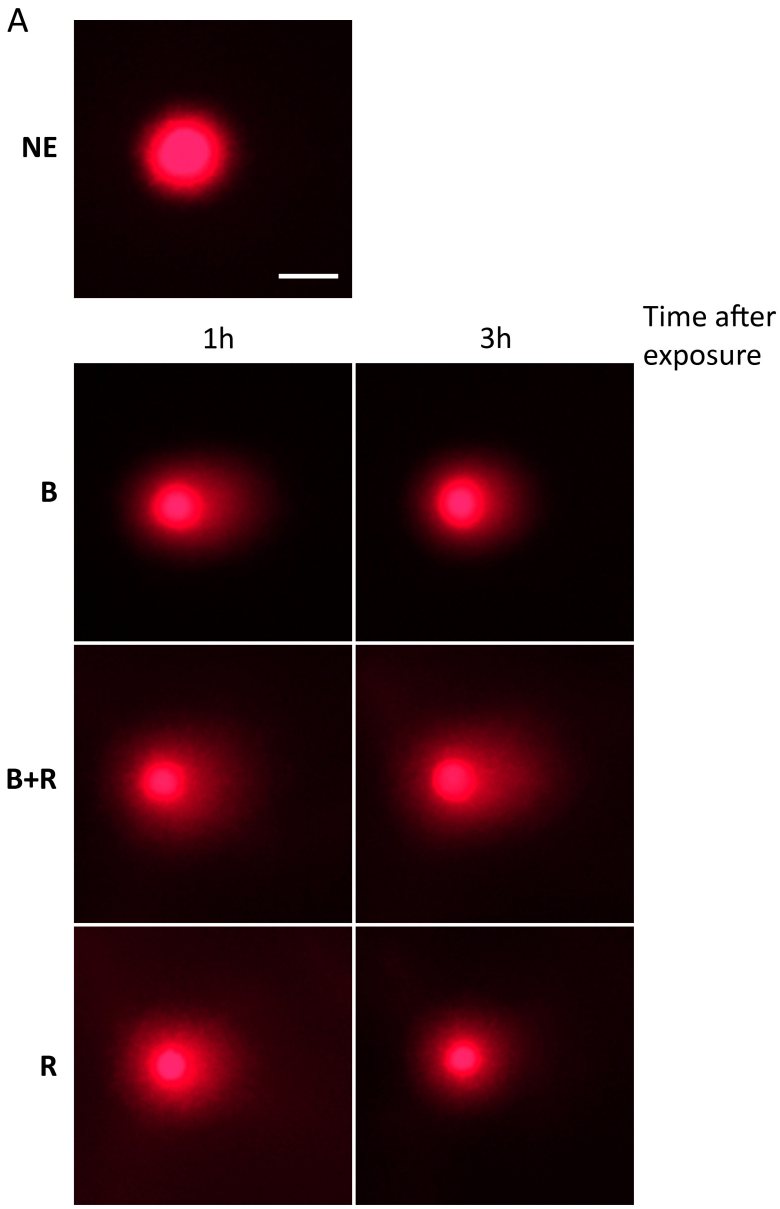
A
NE
1h
3h
Time after exposure
B
B+R
R

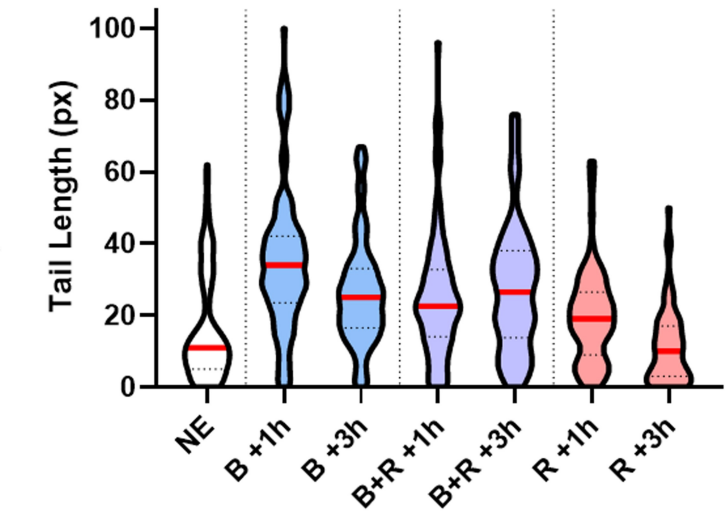
B
Tail Length (px)
100
80
60
40
20
0
NE
B +1h
B +3h
B+R +1h
B+R +3h
R +1h
R +3h

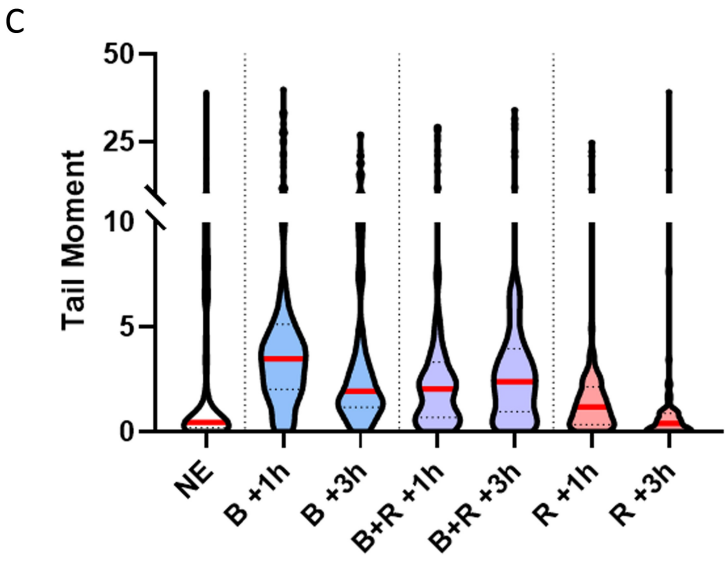
C
Tail Moment
50
25
10
5
0
NE
B +1h
B +3h
B+R +1h
B+R +3h
R +1h
R +3h

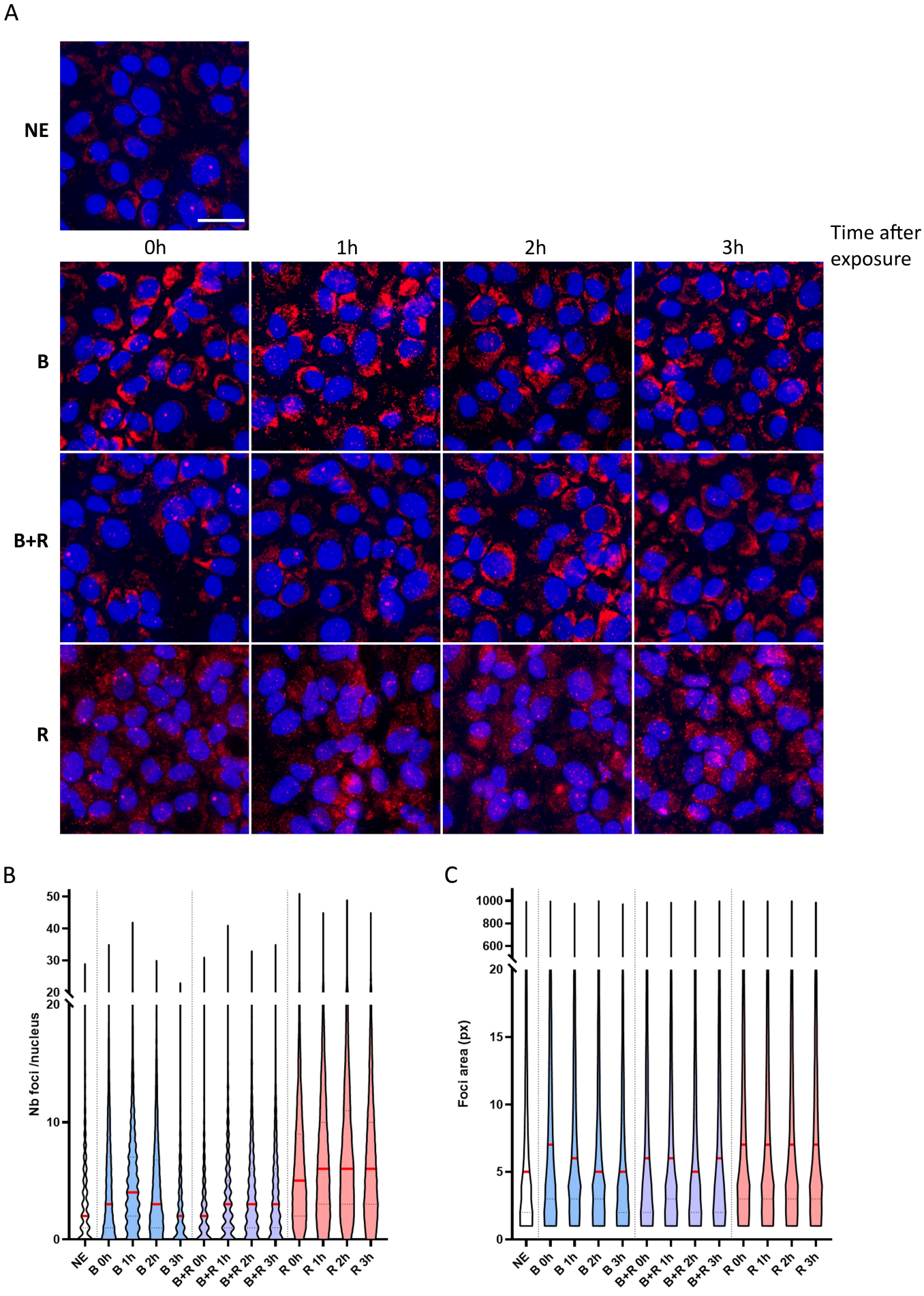
A
NE
0h
1h
2h
3h
Time after exposure
B
B+R
R
B
Nb foci /nucleus
50
40
30
20
20
10
0
NE
B 0h
B 1h
B 2h
B 3h
B+R 0h
B+R 1h
B+R 2h
B+R 3h
R 0h
R 1h
R 2h
R 3h
C
Foci area (px)
1000
800
600
20
15
10
5
0

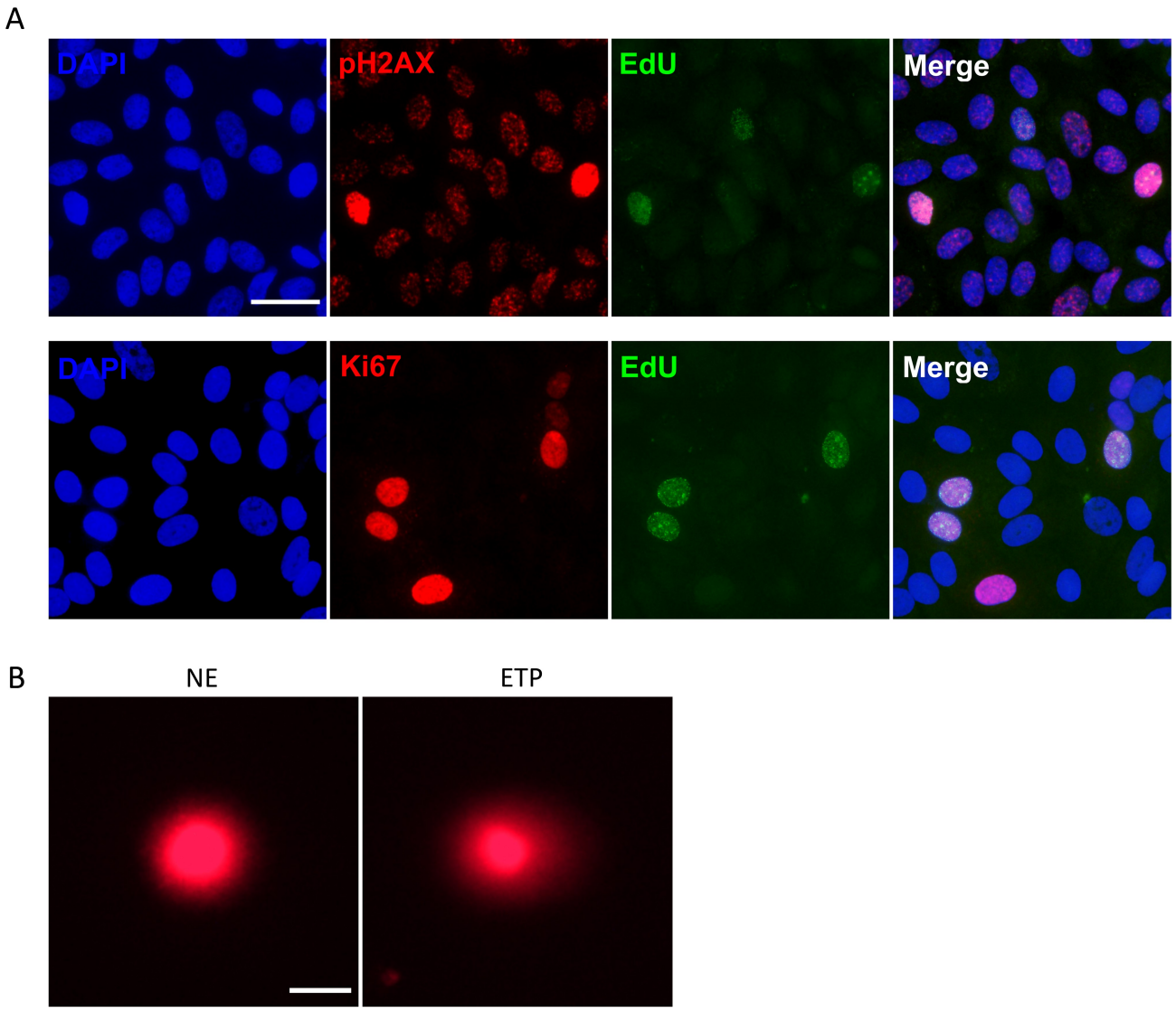

Figure S1: Positive control for DNA damage induction using etoposide (ETP). A. Upper row shows DAPI (blue), anti-γH2AX (red), and EdU (green) staining of BCE cells treated with 100 µM of etoposide for 2h before fixation to induce DNA damage. Lower row shows DAPI (blue), anti-Ki67 (red), and EdU (green) staining. Scale bar= 20 µm. B. Representative comet images of the comet assay for non-exposed cells and cells exposed to etoposide (100 µM for 2h). Scale bar= 20 µm.

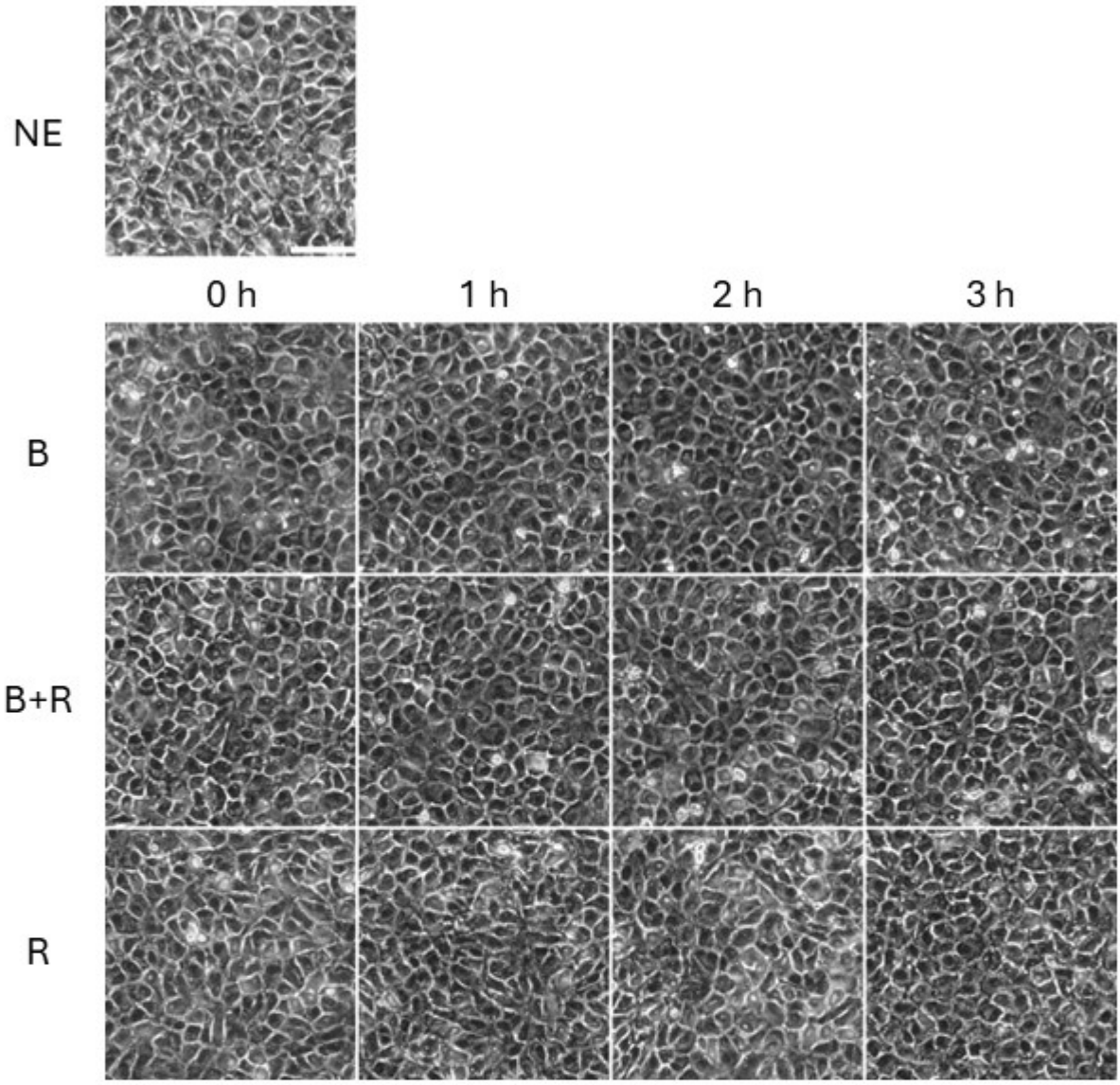

Figure S2: Images of the irradiated cells obtained after fixation with paraformaldehyde. Cells were non exposed (NE) or exposed to blue (B), blue+red (B+R) or red (R) light and fixed at 0, 1, 2 or 3h after exposure. Scale bar= 50 µm.

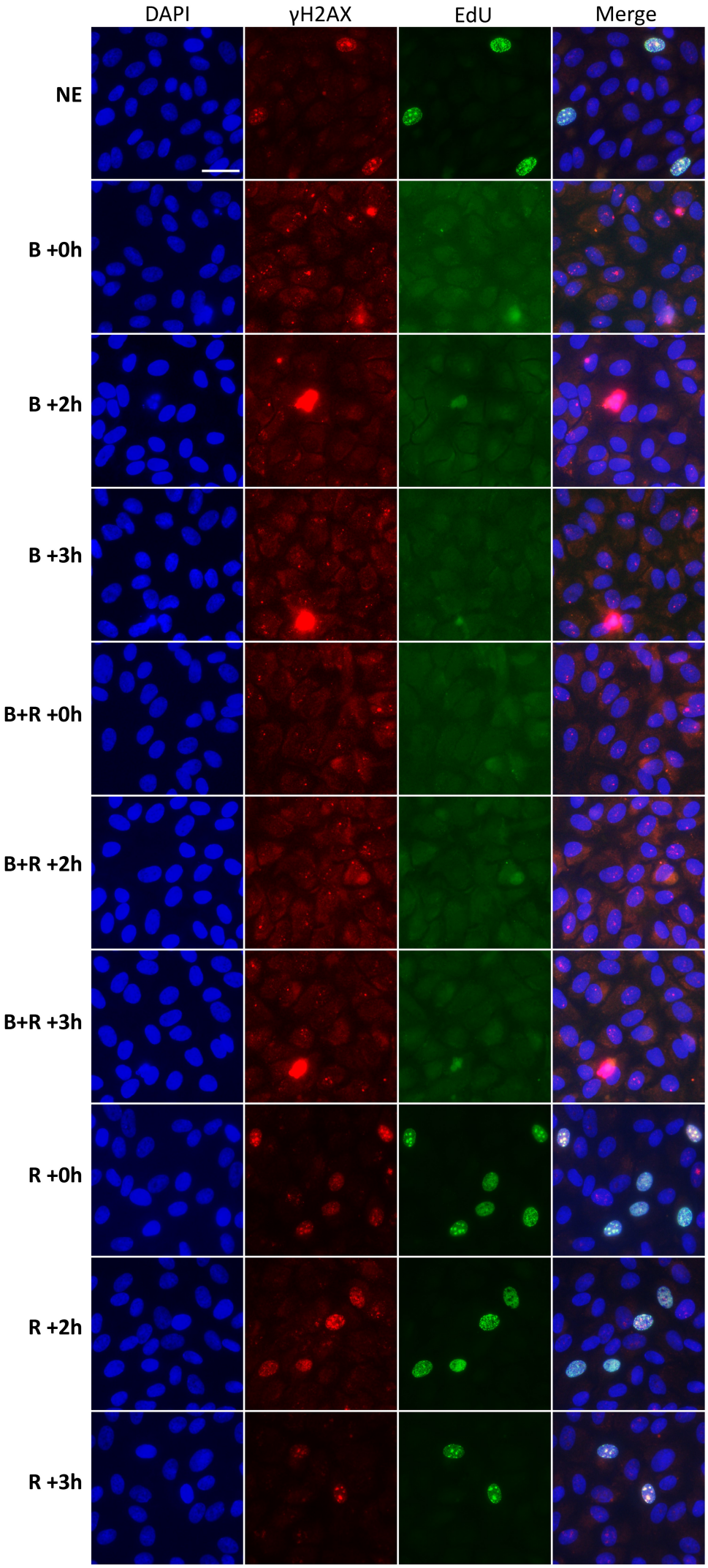

Figure S3: Anti-γH2AX (red), EdU (green) and DAPI (blue) staining of BCE cells exposed to blue (B), blue+red (B+R) or red (R) light, or non-exposed (NE), and fixed at 0, 2 or 3h after exposure. Scale bar= 20 µm.

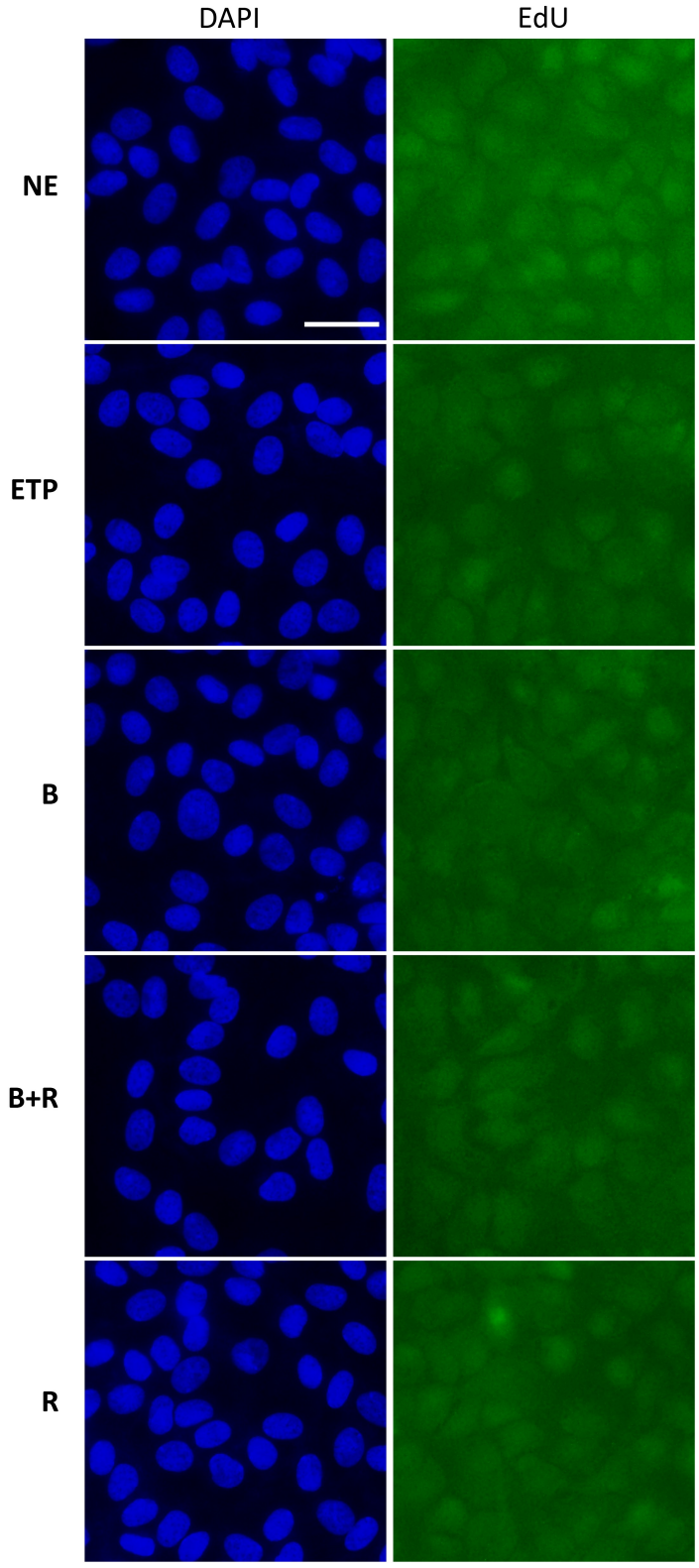

Figure S4: Abscence of replicative cells in confluent BCE cells at passage 6. DAPI (blue), and EdU (green) stainings in BCE cells show the absence of DNA replication in BCE at passage 6 exposed to etoposide (ETP), blue (B), blue+red (B+R) and red (R) LED for 2 h or non-exposed (NE). Scale bar = 20 µm.